

Unexpected Propagation of Ultra-Lean Hydrogen Flames in Narrow Gaps

Fernando Veiga-López^{1,*} Mike Kuznetsov² Daniel Martínez-Ruiz³ Eduardo Fernández-Tarrazo¹
 Joachim Grune⁴ and Mario Sánchez-Sanz^{1,†}

¹*Departamento de Ingeniería Térmica y de Fluidos, Universidad Carlos III de Madrid, 28911 Leganés, Madrid, España*

²*Institut für Kern- und Energietechnik, Karlsruhe Institut für Technologie, 76344 Eggenstein-Leopoldshafen, Deutschland*

³*ETSIAE, Universidad Politécnica de Madrid, Plaza del Cardenal Cisneros 3, 28040 Madrid, España*

⁴*Pro-Science GmbH, Parkstrasse 9, 76275 Ettlingen, Deutschland*

 (Received 20 November 2019; accepted 26 March 2020; published 1 May 2020)

Very lean hydrogen flames were thought to quench in narrow confined geometries. We show for the first time how flames with very low fuel concentration undergo an unprecedented propagation in narrow gaps: H₂-air flames can survive very adverse conditions by breaking the reaction front into isolated flame cells that travel steadily in straight lines or split to perform a fractal-like propagation that resembles the pathway of starving fungi or bacteria. The combined effect of hydrogen mass diffusivity and intense heat losses act as the two main mechanisms that explain the experimental observations.

DOI: 10.1103/PhysRevLett.124.174501

Hydrogen is one of the preferred fuel options because of its high energy density, versatility, and null-CO₂ emissions when it is oxidized to produce energy either in fuel cells or in combustion systems. One of the main concerns of hydrogen-based power generation technology in comparison to conventional hydrocarbons is the potential safety issues associated with the storage, use, and handling of hydrogen [1–3].

The small size of the H₂ molecule brings along a higher permeation of hydrogen through solid walls, especially in nonmetallic containers [4], what significantly increases the risk of undesired leaks [5]. On top of this, its high reactivity, with a lean flammability limit around %H₂ = 4 at Earth's gravity [3,6], and ignition energy as low as 0.02 mJ, 10 times lower than other hydrocarbons [7,8], make hydrogen more prone to undesired deflagrations and explosions when the leak takes place in confined spaces with no ventilation [9]. Furthermore, the dim visible emissions and weak heat radiated from lean hydrogen flames make their detection extremely difficult [10].

Combustion is a complex exothermic chemical process formed by a sequence of elementary reactions involving intermediate species that are created and consumed during the oxidation of the fuel. Conventional hydrogen premixed flames propagate ideally as a continuous front that advances burning the fresh mixture of fuel and oxidizer and leaves hot combustion products behind (ideally, only water vapor) [11]. However, premixed flames are inherently unstable. The viscosity and thermal expansion gradient across the flame front, the competition between heat conduction and mass diffusion in the fluid, the effect of gravity, the interaction with acoustic waves [12,13], and the heat losses [14] fold and stretch the flame altering some of its dynamic and morphological properties [15].

To further investigate the morphology, stability, and safety issues of ultra-lean confined hydrogen-air flames, we modified a previously used experimental setup (Fig. 1) [16] formed by two parallel flat plates disposed vertically and separated a small distance h apart. Previous combustion studies have made use of similar narrow-channel geometries to investigate the onset and development of premixed flame instabilities [17–19]. Here, the faint emissions of fast hydrogen flames require the utilization of Schlieren techniques and high-speed imaging to track the reaction front. The path followed by the flames can be

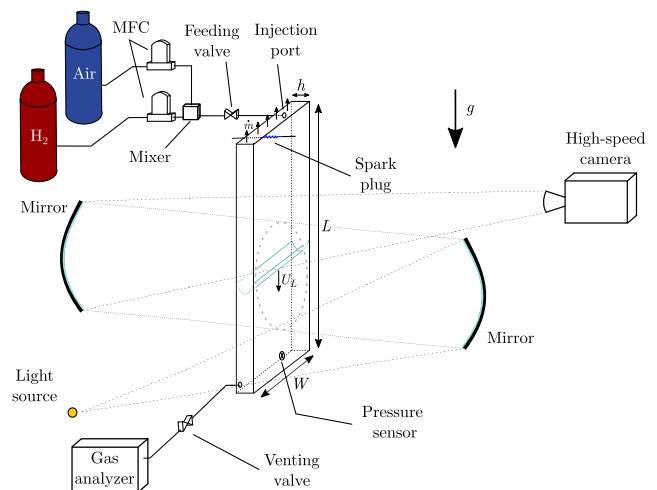


FIG. 1. Schematic of the experimental setup. Z-shape Schlieren system used for image acquisition. The dimensions of the cell are $950 \times 200 \times 6\text{--}1$ mm ($L \times W \times h$). The black arrows at the top end of the chamber represent the unobstructed release of the combustion products.

outlined by trailing the condensed water streaks formed just behind them [20] (Figs. 2 and 3). The small value of the Reynolds number found in our experiments ($Re \approx 33$) anticipates a premixed hydrogen flame that remains in the laminar regime and propagates as a continuous wrinkled front [21]. The high mass diffusivity of hydrogen outlines a reactive front characterized by the formation of small wrinkles related to the development of thermodiffusive instabilities [Figs. 2(a) and 3(a)]. In gaps narrower than $h < 6$ mm, the expected continuous flame front breaks into a set of small flame cells separated by cold, unburned gas, unveiling two unprecedented propagation modes that only emerge in flames with low enough hydrogen concentration. In the first one, the flame front breaks into several unstable flame cells [Figs. 2(b) and 3(b)] that split continuously and propagate leaving a path that conforms a fractal-like pattern that reminds us of ferns and tree leaves. This propagation mode evokes the way starving fungi or bacteria colonies [22,23] spread, with lack of nutrients being analogous to fuel scarcity. Also, diffusion-limited aggregation phenomena reveal similar fractal patterns [24]. In the second regime, the flame front breaks into a few isolated stable flame cells [Figs. 2(c) and 3(c)] that move steadily delineating an almost straight trajectory that reminds us of the fingering patterns found during smoldering combustion of thin solid materials [25].

From the experimental results, it is unclear both how the flame cells are formed and why hydrogen flames withstand more adverse conditions than heavier hydrocarbon fuels [12]. To investigate the causes that lead to the new propagation regimes identified experimentally, we modeled the propagation of the H_2 -air flame using an in-house finite-element code [14]. Since the flow is laminar and the flame thickness $\delta_T \sim (0.5-1)$ mm is comparable to the gap size h , the propagation problem of the flame can be treated as quasi-two-dimensional, considerably simplifying the simulations.

The computations are carried out using an in-house finite-element `FreeFEM++` code that uses a self-adaptive mesh that clusters elements near the reactive front where the maximum gradients of temperature, reaction rate, and velocity are found. The minimum element size used in the calculations is about $1 \mu\text{m}$. The results (Fig. 4) show that increasing the heat losses at the plates leads to a broken reactive front that evolves to form two- or single-headed flame cells, as observed in the experiments for decreasing gap thickness h . The characteristic cell size ranges from 5 to 10 mm for lean hydrogen mixtures (Fig. 4), very similar to the size found in the experimental results (Figs. 2 and 3). Analogous simulations performed for heavier hydrocarbons with less mass diffusivity extinguished at relatively low heat losses forming a continuous reactive front. Our computations, therefore, identified the intense heat losses

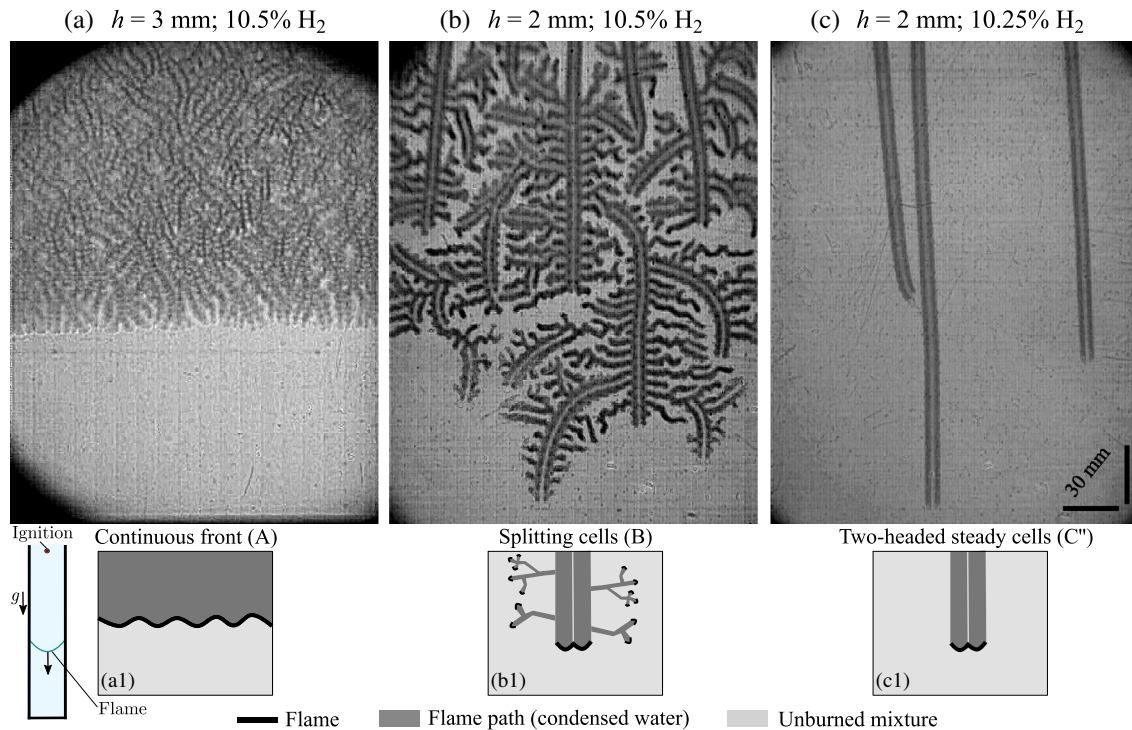


FIG. 2. Downward-propagating hydrogen flames and their different propagation modes. Image and scheme of (a-a1) continuous flame front propagation, (b-b1) splitting cells that propagate forming fractal patterns, and (c-c1) several two-headed isolated steady flame cells. The Supplemental Material [26] includes a video illustrating the three propagation regimes described in the figure.

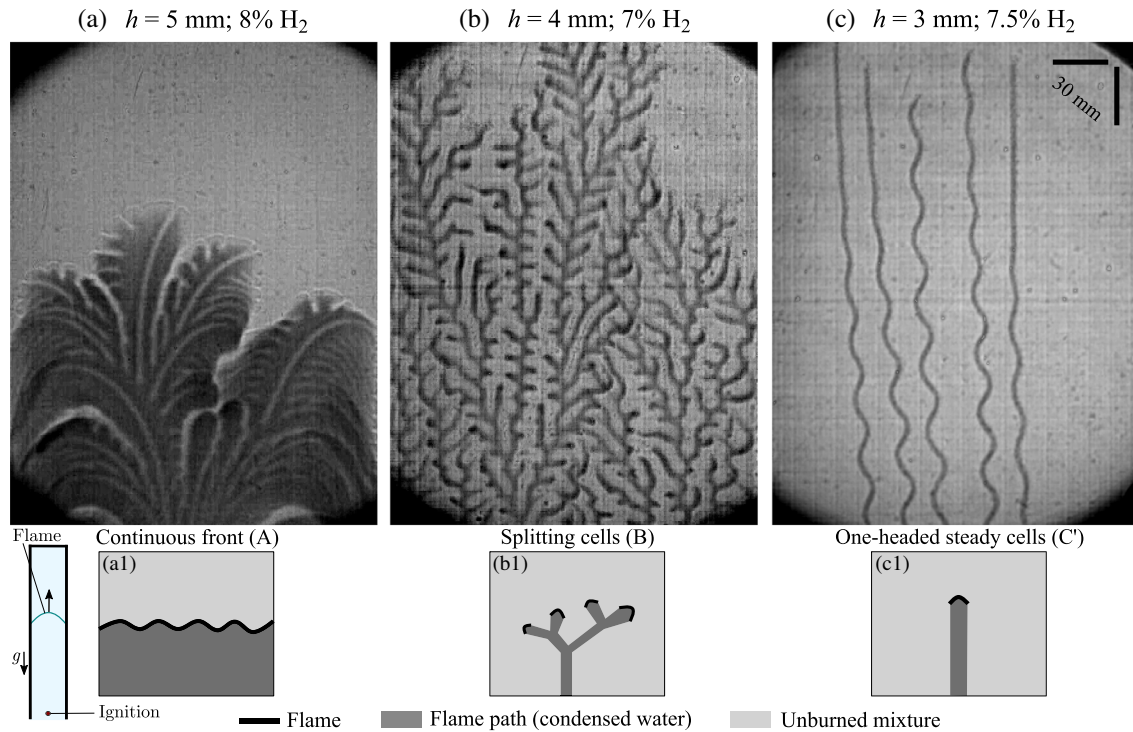


FIG. 3. Upward-propagating hydrogen flames and their different propagation modes. Image and scheme of (a-a1) continuous flame front propagation, (b-b1) fractal-like propagation mode, and (c-c1) several one-headed isolated steady flame cells. The Supplemental Material [26] includes a video illustrating the three propagation regimes described in the figures.

at the walls and the high mass diffusivity of the fuel as the two main mechanisms controlling the emergence of the newly discovered propagation modes (see Supplemental Material [26]).

Experimentally, the relative importance of heat losses is measured using the Peclet number [16] $Pe = h/\delta_T$, a nondimensional parameter that compares the characteristic diffusive and residence times. Lower values of Pe indicate more relevant heat conduction and, therefore, the effect of heat losses can be stimulated by increasing the wall surface area-to-volume ratio reducing the gap size h or thickening the flame by reducing the concentration of hydrogen in the mixture [12,27] (Table S1 in the Supplemental Material [26]). For sufficiently narrow chambers ($h < 6$ mm) and lean mixtures ($\%H_2 < 16$, with slight changes depending on h), conductive heat losses become decisive [12] and the flame front breaks into pieces. It is under these conditions when the two unprecedented propagation regimes appear. Starting with a constant gap size h , we increase the relative importance of heat losses by reducing the concentration of hydrogen. In mixtures leaner than a critical value, the flame evolves from a continuous front to a group of isolated flame cells that propagate as a fractal. Such a transition arises soon after ignition, and the few cells so formed do propagate until they reach the end of the chamber. During this time, the flame cells split and bifurcate cyclically, with newborn flame cells branching off, almost perpendicularly, from the main path to

quench or to later repeat the splitting cycle [Figs. 2(b) and 3(b)]. The paths followed by the flame cells are approximately 5 mm wide and form a unique fractal pattern of fractal dimension $d_f \approx 1.7$ (Supplemental Material [26]) that suggests a nonchaotic behavior of the propagation, similar to the fractal dimension $d_f \approx 1.65$ observed in the propagation of starving bacteria and electrochemical depositions [23,28].

Further reduction in hydrogen concentration triggers a second transition that stops the flame cell splitting mechanism. After ignition, now only a few stable isolated cells travel steadily at an almost constant velocity of around 30 cm/s—case dependent—keeping their size also constant (Supplemental Material [26]) until they reach the end wall of the chamber or extinguish as they collide with the water trail left by another flame cell, where no more fuel is available [Figs. 2(c) and 3(c)]. Conductive heat losses to the walls of the chamber offset heat production to keep the size of the flame cell constant. The unbalance between heat production and heat losses would explain the splitting mechanism observed in richer flames. An analogous behavior is observed in unconfined environments, when radiative heat losses were found to be key for the stabilization of three-dimensional hydrogen flame balls at microgravity [29–31].

The relative importance of heat losses was also modified keeping a constant hydrogen concentration and changing the gap size. Qualitatively, the results are similar regarding the emergence of the two above-described regimes and are

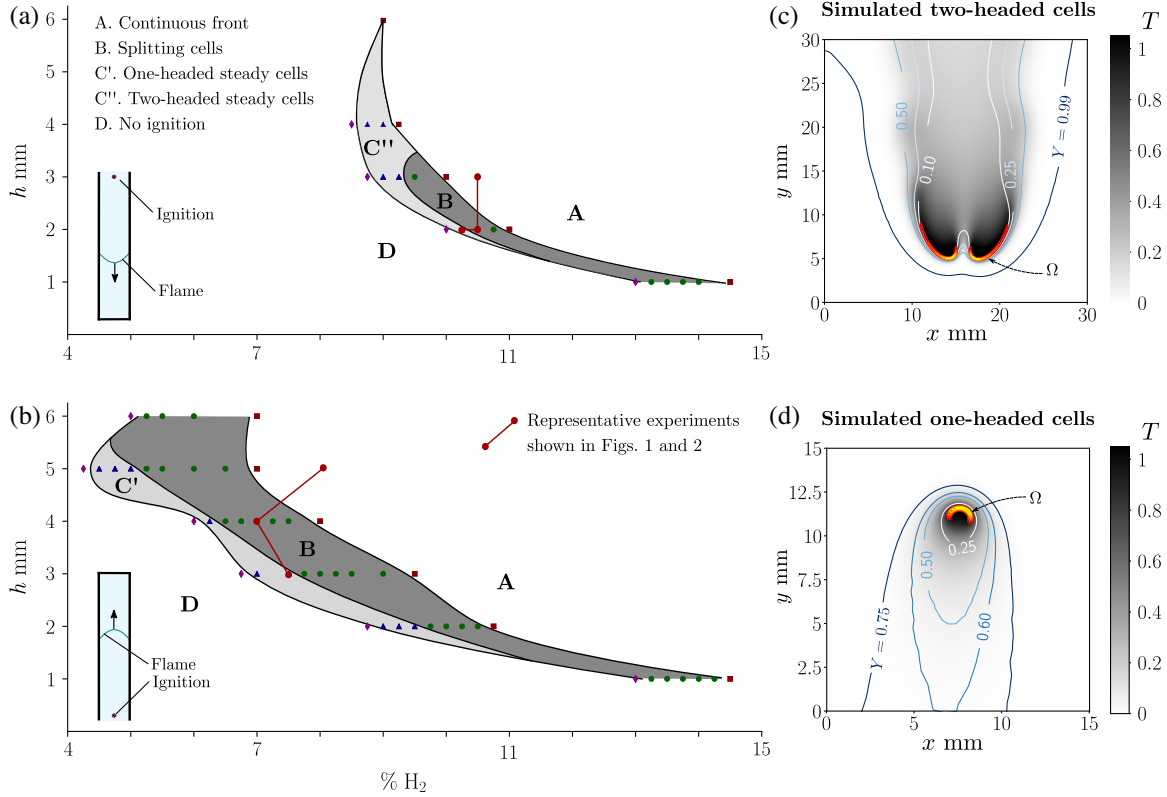


FIG. 4. Flame propagation modes in the h - $\%H_2$ parametric space for both (a) downward- and (b) upward-propagating flames. The solid lines separate the different propagation modes, and the symbols represent the cases actually measured. Every experiment is repeated at least three times to reduce the uncertainty of the measurements. The mixture composition was obtained with an approximate error of ± 0.04 $\%H_2$, and the gap thickness h has an average error of ± 0.114 mm. (c) and (d) detail the single- and double-headed flame cells Ω and the dimensionless temperature field $T = (T' - T_u)/(T_b - T_u)$ obtained from our nonbuoyant numerical computations in the limit of very narrow channels. T' is the local temperature, and T_b represents the adiabatic (equilibrium) flame temperature of the simulated mixtures (Supplemental Material [26]) with $T_u = 298$ K being the ambient temperature.

used to delineate a stability map in the h - $\%H_2$ parametric space (Fig. 4). The criteria used to define the different regions traced in Fig. 4 are based on the fractal dimension of the condensed water path formed during the flame propagation that evolves from $d_f \simeq 2$ [continuous front Figs. 2(c) and 3(a)], $d_f \simeq 1.7$ [splitting cells Figs. 2(b) and 3(b)] to $d_f \simeq 1$ [steady traveling cells Figs. 2(c) and 3(c)]. Also, the fractal dimension provides information about the degree of utilization of the available fuel, with $d_f = 2$ indicating total fuel consumption and $d_f = 1$ showing that most of the fresh mixture remains unburned (Supplemental Material [26]).

The effect of mass diffusivity was explored by testing experimentally methane and dimethylether (DME) flames, fuels with much lower mass diffusivity. The relevant parameter here is the Lewis number Le , a nondimensional number defined as the thermal-to-mass diffusivity ratio that takes the value $Le \approx 0.3, 1, 1.75$ in lean hydrogen, methane, and DME flames, respectively. For methane and DME ($Le \geq 1$), the flame does not withstand the heat losses that increase as the gap size h is reduced and extinguishes from a continuous reactive front. This result

then identifies mass diffusivity as the mechanism that counteracts heat losses [14] and thermodiffusive instabilities triggered by the high diffusivity of hydrogen become the survival mechanism that enables local flame quenching under nonadiabatic conditions and gives birth to flame cells within which the temperature is high enough to sustain combustion [32]. The instantaneous high concentration gradient across the front triggers the fast diffusion of hydrogen from the unburned region toward the surroundings of the flame, increasing the local availability of H_2 and keeping the gas above the crossover temperature ~ 1000 K, the temperature below which the chemical reaction cannot proceed [33–35]. The additional energy released by the burning of this extra fuel is used to counteract conductive heat losses, extending hydrogen combustion toward ultra-lean mixtures below $\%H_2 < 5$.

Gravity also plays an important role in stabilizing or destabilizing flames in vertical channels [15]. To analyze to a greater extent how gravity intervenes in the development of the described propagation modes, we tested experimentally both upward- and downward-propagating flames to expand our stability map (Fig. 4). Similar to methane and

DME flames, in the downward-propagating case, extinction takes place with the H₂ flames forming a continuous reactive front for fuel concentrations below %H₂ < 9 in channels wider than 6 mm, approximately. Surprisingly, leaner mixtures can be found in narrower gaps once the reactive front of the H₂ flame is broken into small separated cells that show, mainly, a double-headed structure similar to that obtained numerically in our computations [Fig. 4(c)]. Simultaneously, the reduction in the gap size increases the relative importance of the gas viscosity, reducing the buoyant velocity induced by gravity and facilitating the propagation of the flame. The minimum fuel concentration %H₂ = 8.5 was found for $h = 4$ mm [Fig. 4(a)].

In upward-propagating flames, buoyancy accelerates the flames and dilates the flammability limits to mixtures significantly leaner than in downward-propagating flames (Fig. 4). As in downward-propagating flames, extinction takes place for richer mixtures in channels wider than $h > 5$ mm. The minimum fuel concentration was found for $h = 5$ mm when a fuel concentration as lean as %H₂ \simeq 4.5 was capable of sustaining a solitary one-headed flame cell [Fig. 4(d)] steadily traveling along the combustion chamber. In narrower channels, conductive heat losses shift the extinction limit toward richer H₂ mixtures (Fig. 4). The influence of gravity diminishes in very narrow channels, with both upward- and downward-propagating flames presenting an almost coincident extinction limit when $h = 1$ mm [Fig. 4(b)]. From the experiments, one can conclude that one- and two-headed flames mainly appear when propagating up and downwards, respectively. However, we found both structures for gravity-free conditions in our simplified numerical model [14], a result that leaves the influence of gravity on the shape of these isolated traveling flames as an open question.

The discovery of the propagation regimes described above opens new research lines regarding near-limit hydrogen combustion in narrow geometries. Based on the experimental results and in the mathematical modeling of the problem carried out in this Letter, we appoint the conductive heat losses to the surrounding walls and the high diffusivity of hydrogen flames as the two physical mechanisms governing the onset of the two propagation regimes unveiled in our Letter. As the use of hydrogen in the near future is expected to increase [1,3], we anticipate a rising concern about the safety of hydrogen-powered devices [16] that will motivate the exploration of interactions between different phenomena. That interest may uncover unknown flame behaviors relevant in the development of safety measures for intentional release or unintentional leakage of hydrogen in narrow gaps and confined environments.

*fveiga@ing.uc3m.es
†mssanz@ing.uc3m.es

- [1] I. Staffell, D. Scamman, A. V. Abad, P. Balcombe, P. E. Dodds, P. Ekins, N. Shah, and K. R. Ward, *Energy Environ. Sci.* **12**, 463 (2019).
- [2] B. Salvi and K. Subramanian, *Renew. Sustain. Energ. Rev.* **51**, 1132 (2015).
- [3] A. L. Sánchez and F. A. Williams, *Prog. Energy Combust. Sci.* **41**, 1 (2014).
- [4] A. Friedrich, J. Grune, T. Jordan, N. Kotchourko, M. Kuznetsov, K. Sempert, and G. Stern, *Safety of Hydrogen as an Energy Carrier* (2009), <https://www.unece.org/fileadmin/DAM/trans/doc/2009/wp29grsp/SGS-6-13e.pdf>.
- [5] V. P. Utgikar and T. Thiesen, *Technol. Soc.* **27**, 315 (2005).
- [6] H. F. Coward and F. Brinsley, *J. Chem. Soc. Trans.* **105**, 1859 (1914).
- [7] R. Ono, M. Nifuku, S. Fujiwara, S. Horiguchi, and T. Oda, *J. Electrostat.* **65**, 87 (2007).
- [8] W. Zhang, X. Gou, and Z. Chen, *Fuel* **187**, 111 (2017).
- [9] D. A. Crowl and Y. Jo, *J. Loss Prev. Process Ind.* **20**, 158 (2007).
- [10] R. W. Schefer, W. D. Kulatilaka, B. D. Patterson, and T. B. Settersten, *Combust. Flame* **156**, 1234 (2009).
- [11] A. Liñán and F. A. Williams, *Fundamental Aspects of Combustion* (Oxford University Press, New York, 1993).
- [12] F. Veiga-López, D. Martínez-Ruiz, E. Fernández-Tarrazo, and M. Sánchez-Sanz, *Combust. Flame* **201**, 1 (2019).
- [13] D. Martínez-Ruiz, F. Veiga-López, and M. Sánchez-Sanz, *Phys. Rev. Fluids* **4**, 100503 (2019).
- [14] D. Martínez-Ruiz, F. Veiga-López, D. Fernández-Galisteo, V. N. Kurdyumov, and M. Sánchez-Sanz, *Combust. Flame* **209**, 187 (2019).
- [15] P. Clavin and G. Searby, *Combustion Waves and Fronts in Flows: Flames, Shocks, Detonations, Ablation Fronts and Explosion of Stars* (Cambridge University Press, Cambridge, England, 2016).
- [16] M. Kuznetsov and J. Grune, *Int. J. Hydrogen Energy* **44**, 8727 (2019).
- [17] J. Sharif, M. Abid, and P. Ronney, in *Premixed-Gas Flame Propagation in Hele-Shaw Cells, Spring Technical Meeting, Joint US Sections* (Combustion Institute, Washington, DC, 1999).
- [18] S. Shen, J. Wongwiwat, and P. Ronney, in *AIAA Scitech 2019 Forum* (2019), p. 2365.
- [19] E. Al Sarraf, C. Almarcha, J. Quinard, B. Radisson, and B. Denet, *Flow Turbul. Combust.* **101**, 851 (2018).
- [20] B. Bregeon, A. S. Gordon, and F. A. Williams, *Combust. Flame* **33**, 33 (1978).
- [21] J. Yanez, M. Kuznetsov, and J. Grune, *Combust. Flame* **162**, 2830 (2015).
- [22] R. Halvorsrud and G. Wagner, *Phys. Rev. E* **57**, 941 (1998).
- [23] E. Ben-Jacob, O. Schochet, A. Tenenbaum, I. Cohen, A. Czirok, and T. Vicsek, *Nature (London)* **368**, 46 (1994).
- [24] T. A. Witten, Jr. and L. M. Sander, *Phys. Rev. Lett.* **47**, 1400 (1981).
- [25] O. Zik, Z. Olami, and E. Moses, *Phys. Rev. Lett.* **81**, 3868 (1998).
- [26] Please see Supplemental Material at <http://link.aps.org/supplemental/10.1103/PhysRevLett.124.174501> for a description of the experimental procedure, properties of the flames and additional details of the flame cells.
- [27] M. Sánchez-Sanz, *Combust. Flame* **159**, 3158 (2012).

- [28] V. Fleury, J. Kaufman, and D. Hibbert, *Nature (London)* **367**, 435 (1994).
- [29] Y. B. Zeldovich, *Theory of Combustion and Detonation in Gases* (USSR Academy of Science, Moscow, 1944).
- [30] P. Ronney, K. Whaling, A. Abbud-Madrid, J. Gatto, and V. Pisowicz, *AIAA J.* **32**, 569 (1994).
- [31] P. D. Ronney, M.-S. Wu, H. G. Pearlman, and K. J. Weiland, *AIAA J.* **36**, 1361 (1998).
- [32] G. Joulin and P. Clavin, *Combust. Flame* **35**, 139 (1979).
- [33] E. Fernández-Tarrazo, A. L. Sánchez, A. Liñán, and F. Williams, *Proc. Combust. Inst.* **33**, 1203 (2011).
- [34] E. Fernández-Tarrazo, A. L. Sánchez, A. Liñán, and F. A. Williams, *Int. J. Hydrogen Energy* **37**, 1813 (2012).
- [35] E. Fernández-Tarrazo, A. L. Sánchez, and F. A. Williams, *Combust. Flame* **160**, 1981 (2013).